Neural transplants in patients with Huntington's disease undergo disease-like neuronal degeneration

F. Cicchetti[a,b,1], S. Saporta[c,d], R. A. Hauser[e], M. Parent[f,g], M. Saint-Pierre[a], P. R. Sanberg[h,i], X. J. Li[j], J. R. Parker[k], Y. Chu[l], E. J. Mufson[l], J. H. Kordower[l], and T. B. Freeman[h,i,1]

[a]Centre de Recherche du CHUL (CHUQ), 2705, Boulevard Laurier, Québec, QC, Canada G1V 4G2; [b]Department of Psychiatry/Neuroscience, Université Laval, Québec, QC, Canada G1K 7P4; [c]Department of Pathology and Cell Biology, [h]Department of Neurosurgery and Brain Repair, [i]Center of Excellence for Aging and Brain Repair, [d]University of South Florida, 2 Tampa General Circle, Tampa, FL 33606-3571; [e]Departments of Neurology; Pharmacology and Experimental Therapeutics, Parkinson's Disease and Movement Disorders National Parkinson's Foundation Center of Excellence, University of South Florida, Tampa, FL 33606; [f]Department of Pathology and Cell Biology; Groupe de recherche sur le système nerveux central; [g]Faculty of Medicine; Université de Montréal, Montreal, QC, Canada; [j]Departments of Genetics and Neurology, Emory University, Atlanta, GA 30322; [k]Department of Pathology, University of Louisville Health Sciences Center, 530 South Jackson Street, Louisville, KY 40202; and [l]Department of Neurological Sciences and Center for Brain Repair, Rush University Medical Center, 1735 West Harrison Street, Chicago, IL 60612

Edited by Solomon H. Snyder, Johns Hopkins University School of Medicine, Baltimore, MD, and approved June 3, 2009 (received for review April 20, 2009)

The clinical evaluation of neural transplantation as a potential treatment for Huntington's disease (HD) was initiated in an attempt to replace lost neurons and improve patient outcomes. Two of 3 patients with HD reported here, who underwent neural transplantation containing striatal anlagen in the striatum a decade earlier, have demonstrated marginal and transient clinical benefits. Their brains were evaluated immunohistochemically and with electron microscopy for markers of projection neurons and interneurons, inflammatory cells, abnormal huntingtin protein, and host-derived connectivity. Surviving grafts were identified bilaterally in 2 of the subjects and displayed classic striatal projection neurons and interneurons. Genetic markers of HD were not expressed within the graft. Here we report in patients with HD that (*i*) graft survival is attenuated long-term; (*ii*) grafts undergo disease-like neuronal degeneration with a preferential loss of projection neurons in comparison to interneurons; (*iii*) immunologically unrelated cells degenerate more rapidly than the patient's neurons, particularly the projection neuron subtype; (*iv*) graft survival is attenuated in the caudate in comparison to the putamen in HD; (*v*) glutamatergic cortical neurons project to transplanted striatal neurons; and (*vi*) microglial inflammatory changes in the grafts specifically target the neuronal components of the grafts. These results, when combined, raise uncertainty about this potential therapeutic approach for the treatment of HD. However, these observations provide new opportunities to investigate the underlying mechanisms involved in HD, as well as to explore additional therapeutic paradigms.

excitotoxicity | inflammation | mutant huntingtin | glutamate | microglia

Huntington's disease (HD) is a progressive, untreatable, and fatal neurodegenerative disorder caused by increased CAG repeats in the *huntingtin* gene (1). The clinical evaluation of neural transplantation as a potential treatment for HD was initiated in an attempt to replace lost neurons and improve patient outcomes (see refs. 2–4). Preclinical rodent and primate experiments demonstrated the feasibility of using embryonic striatal grafts for the treatment of HD. Fetal striatal grafts survive (5), induce behavioral recovery (6, 7), and establish connectivity with the rodent brain (8, 9). Similar results have been reported with xenografts of porcine and human striatal tissue into rodents (2, 9–12). The human striatum is a small enough target to be approached surgically in HD with a realistic goal of achieving confluent graft integration into the host brain (2, 13, 14). Grafts can be functionally integrated (15–18), although such connectivity may not be necessary (19, 20). Similar behavioral results were reported in primate models of HD (21, 22).

The optimal donor age for human striatal graft survival was established in studies using animal models (4, 12, 23, 24). We chose to use embryonic striatal tissue derived from the far lateral portion of the lateral ventricular eminence to optimize striatal-like (P-zone) volume within grafts to greater than 50% (2, 3, 23, 25, 26), which was postulated to correlate with optimal behavioral improvement in rodent models of HD (4, 27–29). Others have used alternative methods of dissection, transplanting the entire ganglionic eminence (4, 30, 31), which includes at least 13 different cell types or nuclei that are not medium spiny neurons of the striatum (23).

Several programs initiated neural transplant trials to evaluate the safety, tolerability, and potential efficacy of human striatal transplantation for the treatment of HD (26, 30–32). Preliminary, open-label studies of neural transplants in patients with HD have demonstrated approximately 2 to 4 years of modest clinical benefits, followed by progressive clinical deterioration similar to the natural history of the disease (31, 32), although there is 1 anecdotal case report of more meaningful clinical benefit (33). The safety profile for neural transplantation in HD may differ significantly from neural transplantation in Parkinson's disease (PD) (32, 34). Neuritic outgrowth of transplanted medium spiny-projection neurons to appropriate host target areas was postulated to mediate graft-derived behavioral benefits (35), although this afferent connectivity of the graft to the host has never been observed at human autopsy (25, 36). Additionally, recent reports of PD-like Lewy-body inclusions within grafts surviving long-term in patients with PD have raised concerns that genetically and immunologically unrelated grafts are susceptible to the disease processes as well (37–39).

The brains of 3 patients with HD who received neuronal transplants a decade earlier were evaluated at autopsy. Patients were clinically monitored, as described previously (31, 32). Here we report in patients with HD that (*i*) graft survival is attenuated long-term; (*ii*) immunologically unrelated grafts degenerate more rapidly than the patient's brain, particularly the projection neuron subtype; (*iii*) cortical neurons project to transplanted striatal neurons; and (*iv*) microglial inflammatory changes in the grafts specifically target the neuronal components of the grafts. We also provide evidence that excitotoxicity and inflammatory mechanisms play a significant role in transplant degeneration and HD as well.

Results

Clinical Outcomes. Autopsy results from patient 2 (W.G.) of our series (32) have been reported previously (25). The evaluations

Author contributions: F.C., P.R.S., and T.B.F. designed research; F.C., S.S., R.A.H., M.P., M.S.-P., J.R.P., Y.C., J.H.K., and T.B.F. performed research; X.J.L. contributed new reagents/analytic tools; F.C., S.S., M.P., R.A.H., Y.C., J.H.K., E.J.M., and T.B.F. analyzed data; and F.C. and T.B.F. wrote the paper.

The authors declare no conflict of interest.

This article is a PNAS Direct Submission.

Freely available online through the PNAS open access option.

[1]To whom correspondence may be addressed. E-mail: Francesca.Cicchetti@crchul.ulaval.ca or tfreeman@health.usf.edu.

This article contains supporting information online at www.pnas.org/cgi/content/full/0904239106/DCSupplemental.

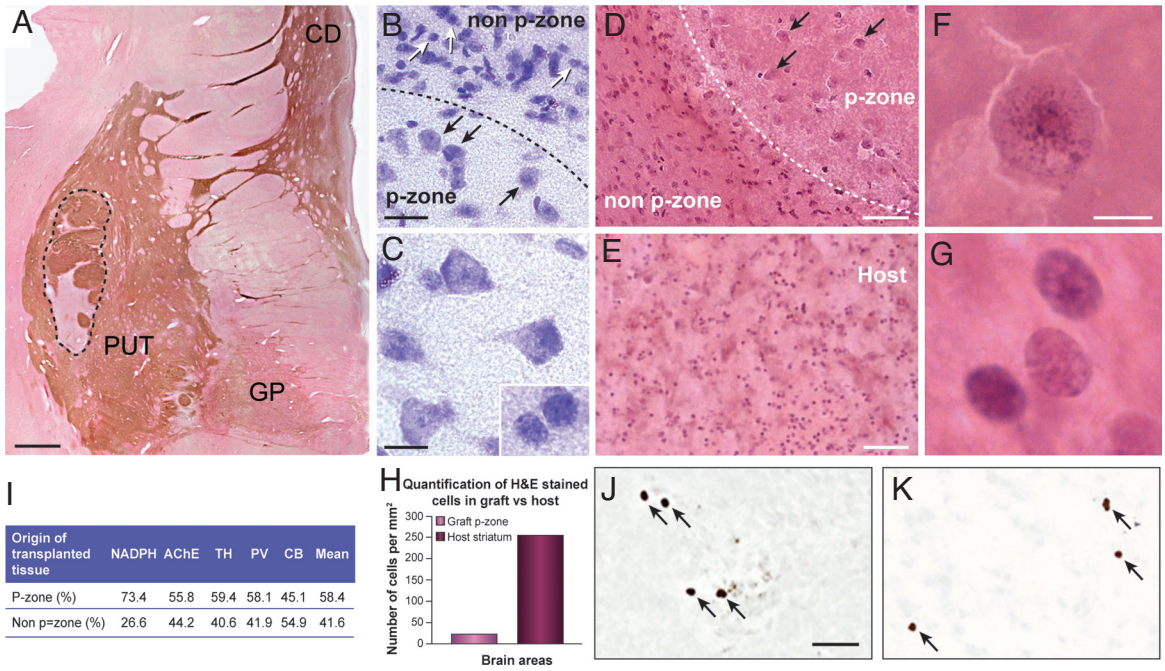

I

Origin of transplanted tissue	NADPH	AChE	TH	PV	CB	Mean
P-zone (%)	73.4	55.8	59.4	58.1	45.1	58.4
Non p=zone (%)	26.6	44.2	40.6	41.9	54.9	41.6

Fig. 1. Graft morphology. (*A*) Low-power magnification of a coronal section stained for AChE, which identifies graft placement within the putamen of the host, at the level of the anterior commissure within the striatum of patient 1. The graft is delineated by a dotted line. P-zone volume was calculated using tissue stained for the striatal markers AChE, NADPH-d, TH, PV and CB (*I*). The mean percentage of P-zone volume per graft was evaluated to be 58% for patient 1 (see *Results* for patient 5). (*B* and *C*) Nissl staining showing the cell density discrepancy between P-zones and non-P-zones (*B*) as well as the notable difference in appearance between cells of the graft (*black arrows* in *B* and also *C*) and of the host (*white arrows* in *B* and *Inset* in *C*). (*D* and *E*) H&E staining also showing the cell-density discrepancies between P-zones and non-P-zones (*D*) as well as in the putamen of the host brain (*E*). Histograms of cell count (per square millimeter of tissue) in grafted P-zones versus host supports the observation of fewer cells within grafted P-zones than in the pathological host putamen (*H*). Note the morphological difference in appearance of cells in the P-zone vs. the non-P-zone (*D*). (*F* and *G*) Higher magnification photomicrographs of individual cells within the P-zone (*F*, and pointed by *black arrows* in *D*) and within the host putamen (*G*). In comparison to cells of the host (*G*), grafted cells appeared larger in diameter, ballooned, and vaculated. Abnormal chromatin deposits exclusively within transplanted cells are discernible using the H&E staining (*F*). These characteristics suggest ongoing grafted neuronal degeneration. The immunostaining for the apoptotic marker caspase-3 (*J* and *K*) revealed equivalent neuronal degeneration in the host and graft. (Scale bars: *A*, 1 mm; *B*, 25 μm; *C* and inset, 12.5 μm; *D* and *E*, 50 μm; *F* and *G*, 6.25 μm; *J* and *K*, 25 μm.) CD, caudate; GP, globus pallidus; PUT, putamen.

reported here correspond to patients 1 (B.L.), 3 (M.C.), and 5 (M.S.) from the same series. Baseline data (age, CAG repeats, symptom duration, time from diagnosis, number of donors, and location of transplants), surgical and immunosuppression methods, clinical outcomes, and complications are described in Tables S1 and S2 and have also been previously described (32). More detailed clinical descriptions are contained in the *SI Text*.

Graft and Striatal Gross Morphology. Macroscopic examination of each patient's brain showed prominent ventricular enlargement and highly atrophied striatal structures. Disease severity (40) was Grade 3 for patients 1 and 3, and Grade 2 for patient 5.

Multiple grafts survived in 2 of the 3 patients (1 and 5). In patient 3, only 1 out of 16 transplants survived (Fig. S1). In patients 1 and 5, grafts were easily identifiable macroscopically and histologically in the host putamen. Complete loss of all caudate grafts was noted in all 3 patients, corresponding to the region where striatal atrophy was most severe. All histological analyses presented here therefore only pertain to patients 1 and 5. Volumetric analysis revealed that grafts replaced 2.9% and 3.8% of the corpus striatum volume of the right and left hemispheres, respectively, of patient 1, and 4.3% of the corpus striatum volume of the left hemisphere of patient 5 (see Fig. S2). The largest graft was identified in the left putamen of patient 1 and measured 39.7 mm^3, similar in size to what was observed in an autopsy performed at 18 months after transplantation (3). Despite preservation of graft volume with time, brain atrophy was notable in all patients. Patient 1 exhibited a 56.5% putamenal shrinkage in comparison to control values and patient 3 demonstrated a 45% putamenal shrinkage, which is consistent with previous autopsy studies reporting a 5% yearly rate of striatal atrophy in HD (41) and a 43 to 47% putamenal atrophy in HD patients in comparison to age-matched controls (42).

Graft Survival and Cellular Composition. Immunohistochemical evaluation of surviving putamenal grafts demonstrated regions with striatal markers (P-zones) interspersed with areas of nonstriatal markers (non P-zones), similar to what was observed in a previous case evaluated 18 months posttransplantation (25). The P-zones of grafts in patient 1 were selectively immunoreactive for various markers of interneuron populations, such as acetylcholinesterase (AChE) (Fig. 1*A*), NADPH-d (Fig. 2 *G* and *H*), parvalbumin (PV) (data not shown), and calretinin (CR) (data not shown), as well as markers of projection neurons such as calbindin (CB) (Fig. 2 *C* and *D*). P-zone areas represented an average of 58.4% of the grafted tissue in patient 1 (see Fig. 1). Graft P-zone volumes in patient 5 averaged 49% of total graft volume (data not shown).

Grafted P-zones had a decreased density of neurons in comparison to both similar P-zones evaluated 18 months posttransplantation (Fig. 2 *E* and *F*) as well as host striatal P-zones (see Fig. 2 *C* and *D*). Surviving grafts did not exhibit the morphology of healthy cells in comparison to grafts 18 months posttransplantation (25). Morphological changes typical of neuronal degeneration in HD were observed in nearly all medium spiny-projection neurons labeled with CB (see Fig. 2). These cells appeared rounded, vacuolated, and lacked structural integrity of the cytoplasm and dendritic arborization. On H&E staining, abnormal chromatin organization could be seen (see Fig. 1*F*). CB immunoreactivity within the graft was also diminished (despite nickel-intensified DAB enhancement used in this study) in comparison to CB immunoreactivity in control regions of this HD brain (see Fig. 2*C*,

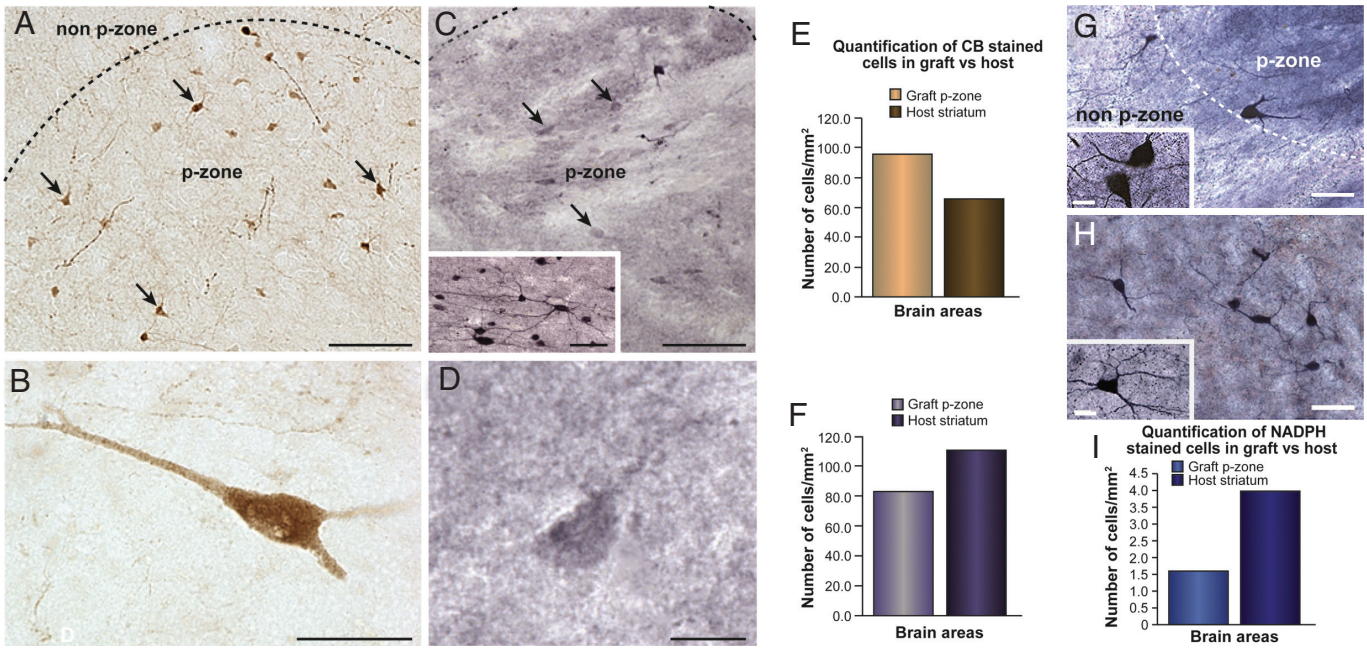

Fig. 2. Comparison of graft health in short- and long-term transplants. Low- (*A*) and high- (*B*) power photomicrographs of CB immunopositive neurons in the P-zone of patient 2, 18 months posttransplantation (25) (revealed with DAB; *brown color*). Because of the reduced CB immunoreactivity seen in the patient 1, (*C* and *D*) 108 months posttransplantation, staining was nickel-intensified, resulting in a purple coloration. In the early stage transplants, the CB-immunoreactive neurons are easily identifiable at lower (*A*) and higher (*B*) magnification within the P-zone by staining intensity, neuronal morphology, and extensive dendritic arborization (*arrows* in *A*). In comparison, CB-immunopositive neurons in late-stage transplants were marked at lower (*C*) and higher (*D*) magnifications by their degenerative appearance, poor CB immunoreactivity, even with nickel-DAB enhancement. These neurons lacked visible cytoplasmic architecture, cell polarity, and dendritic arborization (*arrows* in *C*). Nearly all neurons observed in the grafts of patients 1 and 5 showed similar patterns of staining (data not shown), which contrasted with intense CB staining in cortical regions of the same patients (*Inset C*). (*E*) CB-medium spiny projection neuron counts performed in grafted P-zone vs. host putamen of the short-term transplant recipient demonstrated greater number of cells within the graft than the host (*E*). The opposite finding was observed in patient 1, analyzed a decade posttransplantation (*F*). (*G* and *H*) Higher magnification of NADPH-d staining also exemplifies cell-density discrepancies between grafted P-zone and non-P-zone regions (*G*) and the host putamen (*H*). Insets show high magnification of cells within the graft P-zone (*G*) and host putamen (*H*). (*G*) Histogram of cell counts show a similar decreased cellularity in the grafted P-zone in comparison to the host putamen. (Scale bars: *A* and *C*, 100 μm; *Inset C*, 25 μm; *B*, 25 μm; *D*, 12.5 μm; *G* and *H*, 50 μm; *G* and *H Insets*, 15 μm.)

Inset) as well as in similar grafts at 18 months posttransplantation, where intensification was not necessary (see Fig. 2 *A* and *B*). Caspase-3, a marker of apoptosis, was similarly present in both the graft (see Fig. 1*J*) and the host neurons (see Fig. 1*K*). In comparison, grafted interneurons had a healthier appearance with retained dendritic arborization, and maintained good immunohistological staining (see Fig. 2*G*).

Graft-Induced Inflammatory and Immune Responses. Cluster of differentiation 8 (natural killers and cytotoxic T cells, CD8) (Fig. S3 *a* and *b*), cluster of differentiation 4 (T helper cells, CD4) (Fig. S3 *c* and *d*), and human leukocyte antigen (HLA-DR) (data not shown), were positively identified within the graft, indicating an ongoing immune response at the time of death.

Although astrogliosis typical of HD was observed in the host striatum, the edge of the graft was demarcated by a strong astrocytic response (Fig. 3*A*), where GFAP-positive cells had a morphological appearance of reactive astrocytes. Within the graft itself, the more rarely encountered GFAP cells were recognizable by their nonactivated state (Fig. 3*B*). The pattern of astroglial response respected the boundaries of the solid transplants (Fig. 3*C*).

In contrast to the astrocytic response around the border of the graft, the microglial response differently recognized the P- and non-P-zones within the graft (Fig. 3*D*). In particular, there was activation of microglia within and surrounding those components of the grafts containing striatal markers. Grafted regions lacking striatal markers, which contained immunologically identical donor tissue, were relatively free of microglial activation (see Fig. 3*D*). Activated microglia were frequently intermingled with neuronal nuclei- (NeuN) positive cells and were periodically seen to engulf neuronal elements of the graft, more so on the edge of P-zones than in the host striatum suggestive of potential phagocytosis (Fig. 3 *E*–*G*).

The absence of protein aggregates (ubiquitin) (see Fig. S3*e*) or of abnormal huntingtin protein (EM48) (Fig. S3*g*) within the graft suggest that the transplant was spared from the primary pathological effect of the abnormal *huntingtin* gene. However, ubiquitin (Fig. S3*f*) and EM48 (Fig. S3*h*) were expressed within the host striatum. Additionally, EM48 expression was also pronounced in layer 5 of the cortex (Fig. S3 *i* and *j*).

Host Projections to the Graft. Synaptophysin immunoreactivity was demonstrated in patient 1 (Fig. 4 *A*–*D*), suggesting establishment of synaptic contacts by transplanted neurons. Host-derived dopaminergic fibers grew into the transplant in both cases, as demonstrated by tyrosine hydroxylase (TH) immunohistochemistry (Fig. 4 *E* and *F*). In the striatum, vesicular glutamate transporter 1 (vGlut1)+ axonal varicosities (terminals), found specifically in cortico-striatal axonal projections (43), were observed closely apposed to CB+ neurons in both the host striatum and the transplant (Fig. 4*G*). Electron microscopic examination of the graft P-zone in patient 1 revealed asymmetrical synaptic contacts established by vGlut1 immunolabeled axon varicosities (terminals) (Fig. 4*H*). Technical difficulties in achieving adequate preservation of the fine structure precluded a complete ultrastructural morphological analysis. Of note, the regions within the grafts receiving glutamatergic input colocalized exactly with the regions expressing microglial activation.

Discussion

We have demonstrated that graft survival in patients with HD is attenuated a decade following transplantation. Multiple surviving

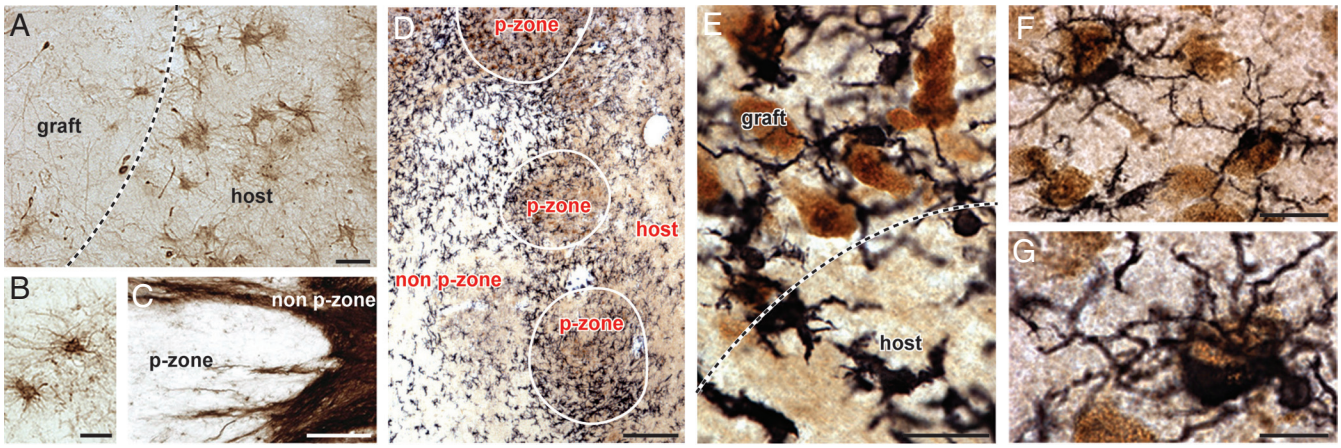

Fig. 3. Inflammatory responses to grafts. Both astrocytosis and microgliosis were evaluated and found to be consistent in all 3 hemispheres; representative photomicrographs of patient 1 are illustrated here. (*A*) The astrocytic response is significant in the host but minimal within the graft, as investigated by GFAP staining. The edge of the graft is demarcated by a particularly strong astrocytic response, characterized by activated astrocytes. A few nonactivated astrocytes are observable within P-zones (*B*). Abundant GFAP fiber staining is seen within the non-P-zone (*C*). These nonactivated astrocytes expressed fibers that extended throughout the non-P-zones but did not significantly invade P-zone. (*D*) Low-power photomicrograph of double immunostaining for the neuronal nuclear marker NeuN (*brown*; DAB chromogen) and the microglial marker Iba-1 (*black*; nickel-DAB chromogen) at the interface of a P-zone and non-P-zone and at the interface of the graft and the host. A pronounced microglial response is demonstrated cuffing the edge of the P-zone as well as within the P-zone. Microglial cuffing is seen predominantly at the interface between P-zones and non-P-zones, as opposed to the interface between the non-P-zone portion of the graft and the host. (*E*) Higher magnification of NeuN/Iba-1 staining at the interface graft/host. (*F* and *G*) Higher power photomicrographs depicting examples of grafted neurons intermingled with microglial cells. Of note, microglial cells were often observed engulfing neuronal elements, resembling an ongoing phagocytic event. (Scale bars: *A*, 25 μm; *B*, 20 μm; *C*, 100 μm; *D*, 300 μm; *E* and *F*, 25 μm; *G*, 12.5 μm.)

grafts were observed in only 2 of our 3 patients. Case 3 (see ref. 32) had only 1 of 16 surviving grafts, which is unusual for any PD or HD transplant recipient using similar techniques (3, 13, 14, 37, 38). Caudate grafts did not survive in any of these HD patients, similar to what we reported 18 months after transplantation (25). Because the caudate displays the greatest neuronal degeneration and astrogliosis in HD, the current findings suggest that this region is a poor transplant niche in this disease. Long-term putamenal grafts had decreased cellularity in comparison to those at 18 months posttransplantation. Grafted cells appeared unhealthy, particularly projection neurons within the grafts. The expression of intraneuronal caspase-3 suggests that striatal cell loss was induced, at least in part, by apoptosis. These results differ significantly from 18-month and 6-year posttransplantation cases where healthy graft survival was reported (25, 36). Neural degeneration at 10 years of neuronal transplant in HD patients is widespread and potentially incompatible with any long-term graft-derived benefit. These results differ from similar case reports in patients with PD (37–39). In those cases, 2 to 8% of transplanted cells demonstrated disease-specific markers (Lewy bodies) (37, 39) and 40 to 80% of dopaminergic neurons and cytoplasmic α-synuclein (38, 39). Despite this, cells were viable, metabolically active (38) and remained differentiated with neuritic reinnervation of the host striatum and with long-term clinical efficacy in individual anecdotal cases (37, 38).

There was diminished cellular viability in all grafted cells at 10 years (vs. 18 months) posttransplantation. Importantly, poor cellular viability was profound in the grafted striatal projection neurons in particular, as opposed to grafted interneurons that still showed distinct cellular cytoarchitecture and polarity but with fewer dendritic extensions than was observed at 18 months posttransplantation. The preferential degeneration of grafted medium-spiny neurons in comparison to interneurons recapitulates the pattern of

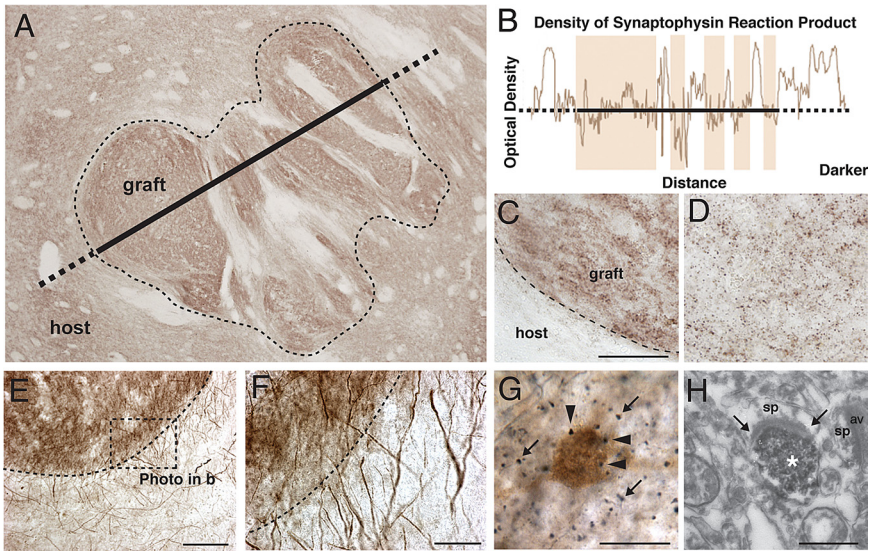

Fig. 4. Graft connectivity. (*A*) Low-power photomicrograph of synaptophysin immunoreactivity inside the graft (*dotted line*). The density of synaptophysin reaction product is depicted in (*B*), in the form of an optical density plot taken along the line shown in (*A*). (*C* and *D*) High magnification of synaptophysin staining in (*C*) a P-zone of the graft and (*D*) in the host striatum. (*E*) Photomicrograph of TH immunostaining of the grafted P-zone (*dotted line*). (*F*) Numerous host-derived TH+ fibers are observed with seamless penetration of the graft border. (*G*) vGlut1 axon varicosities (*black dots*; *arrows* within the neuropile) were found closely apposed to cell bodies labeled for CB (*brown*, *arrowheads*) in both the host striatum and the transplant. (*H*) Example of a vGlut1-labeled axon varicosity (asterix) within the transplant P-zone exhibiting an asymmetrical synaptic contact (*Between small arrows*). (Scale bars: *C* and *D*, 25 μm; *E*, 100 μm; *F*, 25 μm; *G*, 20 μm; *H*, 500 nm.) av, axon varicosity; sp, spine.

striatal cell loss seen in HD, suggesting that disease-like cell loss is also occurring within the genetically unrelated grafts.

Excitotoxicity may play a fundamental role in the degenerative processes seen within these transplants. Glutamatergic axon varicosities from the cerebral cortex were found closely apposed to striatal projection neurons in both the host striatum and the transplants. Within the graft, they were more abundant in the P-zones that contain the neurons that normally receive cortical glutamatergic innervation. Furthermore, microglial infiltration specifically cuffed the P-zones within the grafts, suggesting that microglial activation was responding to specific cues found within the striatal P-zone components of the graft. As the non-P-zone components of the allografts have the same immunological surface antigens as P-zone elements, the selective microglial response to P-zones in particular is compatible with the hypothesis that this response is mediated by neurotoxicity (44, 45) rather than a subacute immune rejection (14). Similar loss of striatal projection neurons is seen following excitotoxicity secondary to glutaric acid in the brains of patients with Glutaric Acidemia Type 1, which leads to an HD-like syndrome in young children (46, 47). In rats, no similar colocalization of glutamatergic input with P-zone-specific microglial infiltration has been described, suggesting that the pathological findings described in the study represent a neurotoxic event. However, it is also possible that the cortex is making appropriate synapses with the graft.

The lack of EM48 (a marker of the abnormal *huntingtin* gene) within grafts, in the presence of robust graft degeneration, indicates that the abnormal HD gene is not required within the striatal neurons to induce degeneration. Instead, the degeneration of striatal grafts may be a remote consequence of the abnormal gene expressed elsewhere in the brain. Among other regions, EM48 was located in layer 5 of the cortex, the origin of the vGlut1 innervation of both the striatum and our transplants. Normal huntingtin immunolabeling has similarly been identified in layer 5 cortico-striatal projection neurons of the normal rat (48). In addition to glutamatergic input to the striatum, cortico-striatal projections also provide trophic support to striatal neurons (49). These data suggest that grafts degenerate secondary to either excitotoxic glutamatergic inputs from the cortex combined with microglial activation against striatal components of the grafts and to the loss of adequate host trophic support. The pattern of graft degeneration that so closely recapitulates the pattern of striatal degeneration in HD suggests that findings in transplantation provide a possible model for the mechanisms of degeneration of the striatum of patients with HD as well.

In the present study, we also observed that the grafts were strikingly more affected by pathological processes than the host striatum, despite the fact that the grafts were young, immunologically unrelated to the patients with HD, and exposed to the disease process for only a decade. Cortical glutamatergic projections to both the graft and the host striatum were demonstrated. At the electron microscopy level, synaptic contacts between glutamatergic axon varicosities and unlabeled dendrites within the graft were also observed. It is possible that the immune responses to solid grafts in the absence of immunosuppression (14, 50), combined with the release of glutamate directly from microglia or glutamatergic cortico-striatal afferents, accelerated the degeneration process in grafted vs. host striatal neurons, as suggested in animal studies (51). Graft degenerative changes seen here are incompatible with clinical benefits after 10 years, vs. PD, where only 2 to 8% of grafted cells have α-synuclein inclusions (37–39), and clinical benefits lasted for 11 to 12 years in those patients (37, 38).

It has been postulated that if striatal transplants are to be effective for the treatment of HD, they need to prevent local neuronal degeneration within the striatum (26) as well as widespread degeneration of cortical afferents projecting to the grafts (2–4, 35). However, meaningful neuritic outgrowth was not demonstrated in either the present study or previous studies of grafts surviving 18 months (25) or 6 years posttransplantation (36). The volume of striatal loss in our transplant recipients is similar to what has been described in other patients with HD (42). Therefore, the present study failed to demonstrate that embryonic striatal grafts slowed degeneration of the surrounding striatum via either neuritic outgrowth or graft-derived neurotrophic expression (35). However, the present study demonstrated that glutamatergic cortico-striatal projections terminate onto transplanted striatal components of the grafts. The functional significance of this interaction remains unknown. Rather than the grafts positively influencing the cortex, the pathology within the cortex appeared to induce neuronal degeneration within the grafts.

Risks associated with neuronal transplantation in this study are not trivial. Two subjects developed a total of 3 subdural hematomas that required surgical evacuation, out of a total of 14 hemispheric transplants (32). This was likely because of cerebrospinal fluid loss in the setting of brain atrophy leading to the formation of hygromas, which frequently convert to hematomas. This also led to a targeting error in the last needle tract in 1 patient. This safety profile differs dramatically from that observed in transplant recipients with PD, where the same surgeon (T.B.F.) had no surgically relevant subdural hematomas in 66 consecutive transplant procedures (32). Based on these results, it is our impression that any future surgical therapy for HD should intervene in earlier stage patients with less brain atrophy, and minimize cerebrospinal fluid loss to diminish the risks of subdural hematomas and targeting errors.

Clinical efficacy has been postulated to require that greater than 50% of grafted volume is composed of P-zones (4, 27, 29) that contain striatal projection neurons. This anatomical threshold was achieved in both the present and our previous study (3). However, clinical efficacy in our patients was mild in magnitude, short-lived, subject to the limitations of small open-label trials (placebo effect, as well as potential investigator and subject bias), and did not prevent the unremitting and fatal progression of HD. Similar clinical outcomes have been reported by others (31), despite the fact that their grafts were derived from a much more nonspecific dissection of the striata in their first autopsy report (53). These similar clinical results, using significantly different dissection methods with a "subthreshold" quantity of P-zones within grafts, suggests that clinical benefits, if any, are the result of nonspecific effects of these grafts (19, 20). The combination of an unfavorable risk-benefit profile, short-term and mild benefits at best, and significant disease-like graft degeneration makes future trials of fetal-cell transplantation using these techniques potentially unwarranted. Therapeutic strategies (with or without neural grafts) aimed at altering inflammatory or immune responses, host-derived neurotoxicity, and neurotrophic support in the brain may prove to be more promising for the future treatment of HD.

Methods

Donor Tissue Preparation and Transplantation. Methods for tissue preparation, neuronal transplantation, immunosuppression, location of the transplants, number of donors per patient, and clinical genetic as well as radiologic evaluation have been described previously (3, 23, 25, 32). Solid-tissue transplants measuring 0.5 to 1 mm^3 were derived from the far lateral portion of the lateral ventricular eminence to optimize the percentage of tissue of striatal origin (23). All patients received transplants into both the caudate and putamen derived from 5 to 8 striatal primordia per site. The 3 patients in this series represent patients 1, 3, and 5 from our clinical report (32).

Postmortem Tissue Preparation and Histological Evaluation. Postmortem intervals were 5, 4, and 5 h for patients 1, 3, and 5 respectively. The brains were bisected, cut serially into 1-cm slabs in a coronal plane and immersed in Zamboni's fixative (25) for 8 days at 4 °C. The brain of patient 5 was collected in the same fashion as patients 1 and 3, but only one-half of the brain was immersed in Zamboni's solution. The other half was immersion-fixed in 4% glutaraldehyde prepared in cacodylate buffer for electron microscopic examination. Following the 8-day fixation period, brain slabs were then placed in a 20% sucrose in 0.1 M PB cryoprotectant solution until they sank and were cut frozen into 40-μm thick sections.

Series of adjacent sections were processed for histochemical and immunohistochemical (see *Supplemental Methods* in *SI Text* for protocol details) analyses for the visualization of H&E (brain cytoarchitecture) and various striatal subtypes of interneurons; NADPH-d (marker for nitric oxide containing striatal interneurons),

AChE (enzyme catalyzing hydrolysis of the neurotransmitter acetyl choline in cholinergic neurons), PV (Sigma; 1:1,000) or CR (Swant; 1:2,500). The immune/inflammatory response was investigated using GFAP (astrocytes; Dako Canada; 1:2,500), CD4 (T helper cells; Serotec; 1:250), CD8 (natural killers and cytotoxic T cells; Serotec; 1:200), HLA-DR (surface antigen of class II major histocompatibility complex; Serotec; 1:200), while other sections were processed for double immunohistochemistry to visualize the microglial response (Iba-1; Wako Chemicals; 1:1,000) to grafted neuronal elements (NeuN; Chemicon; 1:2500). Genetic markers of huntingtin were evaluated using EM48 (abnormal huntingtin protein; provided by X.J. Li, Emory University; 1:2,000) and ubiquitin (Calbiochem; 1:250). Finally, host-derived connectivity was assessed by TH (Pel-Freez; 1:1,000), synaptophysin (Calbiochem; 1:500), double immunostaining for CB (striatal projection neurons; Sigma; 1:2,500), and vGlut1 (cortico-striatal projections; Sigma; 1:500), and electron microscopy (see *Supplemental Methods* in *SI Text* for protocol details). Sections intended for electron microscopy were prepared as above for vGlut1 immunohistochemistry, but for single immunostaining were prepared only using a slightly modified version of previously published protocol (52).

Three-Dimensional Reconstruction, Striatal P-Zone Evaluation and Cell Counts. Three-dimensional reconstruction was performed using the Serial Section Reconstruction method provided by the Neurolucida software, version 6.0 (Microbrightfield) on Nissl-stained sections. Volumetric evaluation of graft size (Cavalieri method) as well as P-zone/non-P-zone areas for patients 1 and 5 were explicitly performed using the right hemisphere of both patients 1 and 5. Both grafts and P-zones were delineated using Nissl staining and the Tracing Contours option in the Stereo Investigator software, version 5.0 (Microbrightfield). Areas for either P-zones or non-P-zones were calculated using Contour Measurements option. Cell counts were performed using the Optical Fractionator probe (Stereo Investigator software) based on 3 different immunostaining markers for NADPH (interneurons), H&E (general cell marker), and CB (projection neurons). More details on the assessment of graft volume, estimation of striatal P-zones, and 3-dimensional reconstruction are provided in *SI Text*.

ACKNOWLEDGMENTS. The authors thank Dr. Peter Gould of the service d'anatomopathologie et cytologie, Hôpital de l'Enfant-Jésus, Québec, Canada for pathological diagnosis, and clinical coordinators Deborah Scott and Holly Delgado for their commitment and expertise. This work was supported in part by the Huntington Society Canada, the Fondation Canadienne pour l'Innovation (F.C.), and Tampa General Healthcare, the International Organization of Glutaric Acidemia (T.B.F.).

1. Huntington's Disease Collaborative Research Group (1993) A novel gene containing a trinucleotide repeat that is expanded and unstable on Huntington's disease chromosomes. *Cell* 72:971–983.
2. Freeman TB, Hauser RA, Sanberg PR, Saporta S (2000) Neural transplantation for the treatment of Huntington's disease. *Prog Brain Res* 127:405–411.
3. Freeman TB, et al. (2000) Transplantation of human fetal striatal tissue in Huntington's disease: rationale for clinical studies. Neural transplantation in neurodegenerative disease: current status and new directions. *Novartis Found Symp* 231:129–144.
4. Peschanski M, Cesaro P, Hantraye P (1995) Rationale for intrastriatal grafting of striatal neuroblasts in patients with Huntington's disease. *Neuroscience* 68:273–285.
5. Schmidt RH, Bjorklund A, Stenevi U (1981) Intracerebral grafting of dissociated CNS tissue suspensions: a new approach for neuronal transplantation to deep brain sites. *Brain Res* 218:347–356.
6. Deckel AW, Robinson RG, Coyle JT, Sanberg PR (1983) Reversal of long-term locomotor abnormalities in the kainic acid model of Huntington's disease by day 18 fetal striatal implants. *Eur J Pharmacol* 93:287–288.
7. Isacson O, Brundin P, Kelly PA, Gage FH, Bjorklund A (1984) Functional neuronal replacement by grafted striatal neurones in the ibotenic acid-lesioned rat striatum. *Nature* 311:458–460.
8. Pritzel M, Isacson O, Brundin P, Wiklund L, Bjorklund A (1986) Afferent and efferent connections of striatal grafts implanted into the ibotenic acid lesioned neostriatum in adult rats. *Exp Brain Res* 65:112–126.
9. Wictorin K (1992) Anatomy and connectivity of intrastriatal striatal transplants. *Prog Neurobiol* 38:611–639.
10. Deacon TW, Pakzaban P, Isacson O (1994) The lateral ganglionic eminence is the origin of cells committed to striatal phenotypes: neural transplantation and developmental evidence. *Brain Res* 668:211–219.
11. Isacson O, et al. (1995) Transplanted xenogeneic neural cells in neurodegenerative disease models exhibit remarkable axonal target specificity and distinct growth patterns of glial and axonal fibres. *Nat Med* 1:1189–1194.
12. Wictorin K, Brundin P, Gustavii B, Lindvall O, Bjorklund A (1990) Reformation of long axon pathways in adult rat central nervous system by human forebrain neuroblasts. *Nature* 347:556–558.
13. Kordower JH, et al. (1995) Neuropathological evidence of graft survival and striatal reinnervation after the transplantation of fetal mesencephalic tissue in a patient with Parkinson's disease. *N Engl J Med* 332:1118–1124.
14. Kordower JH, et al. (1997) Fetal grafting for Parkinson's disease: expression of immune markers in two patients with functional fetal nigral implants. *Cell Transplant* 6:213–219.
15. Campbell K, Wictorin K, Bjorklund A (1995) Neurotransmitter-related gene expression in intrastriatal striatal transplants–I. Phenotypical characterization of striatal and non-striatal graft regions. *Neuroscience* 64:17–33.
16. Campbell K, Wictorin K, Bjorklund A (1995) Neurotransmitter-related gene expression in intrastriatal striatal transplants–II. Characterization of efferent projecting graft neurons. *Neuroscience* 64:35–47.
17. Pakzaban P, Deacon TW, Burns LH, Isacson O (1993) Increased proportion of acetylcholinesterase-rich zones and improved morphological integration in host striatum of fetal grafts derived from the lateral but not the medial ganglionic eminence. *Exp Brain Res* 97:13–22.
18. Sirinathsinghji DJ, Heavens RP, Torres EM, Dunnett SB (1993) Cholecystokinin-dependent regulation of host dopamine inputs to striatal grafts. *Neuroscience* 53:651–663.
19. Norman AB, Lehman MN, Sanberg PR (1989) Functional effects of fetal striatal transplants. *Brain Res Bull* 22:163–172.
20. Sanberg PR, Koutouzis TK, Freeman TB, Cahill DW, Norman AB (1993) Behavioral effects of fetal neural transplants: relevance to Huntington's disease. *Brain Res Bull* 32:493–496.
21. Hantraye P, Riche D, Maziere M, Isacson O (1992) Intrastriatal transplantation of cross-species fetal striatal cells reduces abnormal movements in a primate model of Huntington disease. *Proc Natl Acad Sci USA* 89:4187–4191.
22. Isacson O, Riche D, Hantraye P, Sofroniew MV, Maziere M (1989) A primate model of Huntington's disease: cross-species implantation of striatal precursor cells to the excitotoxically lesioned baboon caudate-putamen. *Exp Brain Res* 75:213–220.
23. Freeman TB, Sanberg PR, Isacson O (1995) Development of the human striatum: implications for fetal striatal transplantation in the treatment of Huntington's disease. *Cell Transplant* 4:539–545.
24. Naimi S, Jeny R, Hantraye P, Peschanski M, Riche D (1996) Ontogeny of human striatal DARPP-32 neurons in fetuses and following xenografting to the adult rat brain. *Exp Neurol* 137:15–25.
25. Freeman TB, et al. (2000) Transplanted fetal striatum in Huntington's disease: phenotypic development and lack of pathology. *Proc Natl Acad Sci USA* 97:13877–13882.
26. Freeman TB, et al. (1998) *Human Fetal Tissue Transplantation for the Treatment of Movement Disorders.* (AANS Publications Committee, New York) pp 177–192.
27. Brundin P, Fricker RA, Nakao N (1996) Paucity of P-zones in striatal grafts prohibit commencement of clinical trials in Huntington's disease. *Neuroscience* 71:895–897.
28. Nakao N, Grasbon-Frodl EM, Widner H, Brundin P (1996) DARPP-32-rich zones in grafts of lateral ganglionic eminence govern the extent of functional recovery in skilled paw reaching in an animal model of Huntington's disease. *Neuroscience* 74:959–970.
29. Peschanski M, Cesaro P, Hantraye P (1996) What is needed versus what would be interesting to know before undertaking neural transplantation in patients with Huntington's disease. *Neuroscience* 71:899–900.
30. Bachoud-Levi A, et al. (2000) Safety and tolerability assessment of intrastriatal neural allografts in five patients with Huntington's disease. *Exp Neurol* 161:194–202.
31. Bachoud-Levi AC, et al. (2006) Effect of fetal neural transplants in patients with Huntington's disease 6 years after surgery: a long-term follow-up study. *Lancet Neurol* 5:303–309.
32. Hauser RA, Sandberg PR, Freeman TB, Stoessl AJ (2002) Bilateral human fetal striatal transplantation in Huntington's disease. *Neurology* 58:1704, author reply 1704.
33. Reuter I, et al. (2008) Long-term clinical and positron emission tomography outcome of fetal striatal transplantation in Huntington's disease. *J Neurol Neurosurg Psychiatry* 79:948–951.
34. Kopyov OV, Jacques S, Lieberman A, Duma CM, Eagle KS (1998) Safety of intrastriatal neurotransplantation for Huntington's disease patients. *Exp Neurol* 149:97–108.
35. Watts C, Dunnett SB (2000) Towards a protocol for the preparation and delivery of striatal tissue for clinical trials of transplantation in Huntington's disease. *Cell Transplant* 9:223–234.
36. Keene CD, et al. (2007) Neural transplantation in Huntington disease: long-term grafts in two patients. *Neurology* 68:2093–2098.
37. Kordower JH, Chu Y, Hauser RA, Freeman TB, Olanow CW (2008) Lewy body-like pathology in long-term embryonic nigral transplants in Parkinson's disease. *Nat Med* 14:504–506.
38. Kordower JH, Olanow CW, Hauser R, Chu Y, Freeman TB (2008) Transplanted dopaminergic neurons develop PD pathologic changes: A second case report. *Movement Disorders* 23:2303–2306.
39. Li JY, et al. (2008) Lewy bodies in grafted neurons in subjects with Parkinson's disease suggest host-to-graft disease propagation. *Nat Med* 14:501–503.
40. Vonsattel JP, et al. (1985) Neuropathological classification of Huntington's disease. *J Neuropathol Exp Neurol* 44:559–577.
41. Henley SM, et al. (2006) Increased rate of whole-brain atrophy over 6 months in early Huntington disease. *Neurology* 67:694–696.
42. Mann DM, Oliver R, Snowden JS (1993) The topographic distribution of brain atrophy in Huntington's disease and progressive supranuclear palsy. *Acta Neuropathol* 85:553–559.
43. Raju DV, Smith Y (2005) *Differential Localization of Vesicular Glutamate Transporters 1 and 2 in the Rat Striatum.* (Springer Science and Business Media, New York) pp. 601–610.
44. Biber K, Neumann H, Inoue K, Boddeke HW (2007) Neuronal ''On'' and ''Off'' signals control microglia. *Trends Neurosci* 30:596–602.
45. Conforti L, Adalbert R, Coleman MP (2007) Neuronal death: where does the end begin? *Trends Neurosci* 30:159–166.
46. Flott-Rahmel B, et al. (1997) Nerve cell lesions caused by 3-hydroxyglutaric acid: a possible mechanism for neurodegeneration in glutaric acidaemia I. *J Inherit Metab Dis* 20:387–390.
47. Funk CB, et al. (2005) Neuropathological, biochemical and molecular findings in a glutaric acidemia type 1 cohort. *Brain* 128:711–722.
48. Fusco FR, et al. (1999) Cellular localization of huntingtin in striatal and cortical neurons in rats: lack of correlation with neuronal vulnerability in Huntington's disease. *J Neurosci* 19:1189–1202.
49. Canals JM, et al. (2001) Expression of brain-derived neurotrophic factor in cortical neurons is regulated by striatal target area. *J Neurosci* 21:117–124.
50. Redmond DJ, Vinuela A, Kordower J, Isacson O (2008) Influence of cell preparation and target location on the behavioral recovery after striatal transplantation of fetal dopaminergic neurons in a primate model of Parkinson's disease. *Neurobiol Dis* 29:103–116.
51. Stack EC, et al. (2007) Neuroprotective effects of synaptic modulation in Huntington's disease R6/2 mice. *J Neurosci* 27:12908–12915.
52. Parent M, Descarries L (2008) Acetylcholine innervation of the adult rat thalamus: distribution and ultrastructural features in dorsolateral geniculate, parafascicular, and reticular thalamic nuclei. *J Comp Neurol* 511:678–691.
53. Capetian P, et al. (2009) Histological findings on fetal striatal grafts in a Huntington's disease patient early after transplantation. *Neuroscience* 160:661–675.